Materials Advances

ROYAL SOCIETY OF CHEMISTRY

PAPER

View Article Online
View Journal | View Issue

Cite this: *Mater. Adv.*, 2020, **1**, 3460

Green synthesis of Zn-doped *Catharanthus Roseus* nanoparticles for enhanced anti-diabetic activity

Nagaraj Govindan,[a] Kowsalya Vairaprakasam,[a] Chandraleka Chinnasamy,[a] Tamilarasu Sivalingam[b] and Mustafa K. A. Mohammed *[c]

Recently, many studies have been interested in the bio-production of zinc oxide nanoparticles (ZnO-NPs) for biomedical applications using plants. However, green synthesized zinc-based nanoparticles (Zn-NPs) have not been reported previously. In this research, for the first time, we have prepared eco-friendly Zn-doped *Catharanthus Roseus* (*C. roseus*) plants using a facile photon induced method (PIM) for green biomaterials. Most importantly, the presence of phytoconstituents in the leaf extract of *C. roseus* plays a vital role in the development of NPs, as the phytoconstituents serve as reducing agents, which can be efficiently used for enhanced anti-diabetic performance. X-ray diffraction (XRD) and energy dispersive spectroscopy (EDX) results confirmed the fabrication of the biosynthesized Zn-doped *C. roseus* plant. The prepared NPs revealed high crystallinity with a shifted band gap energy of 2.74 eV in the visible region. Fourier transform infrared spectroscopy (FTIR) showed Zn-doped *C. roseus* surfaces decorated with functional groups. The transmission electron microscopy (TEM) images showed that the NPs are uniformly dispersed in a spherical shape with sizes ranging from 10 to 20 nm. In addition, an alpha-amylase inhibitory assay was employed to assess the anti-diabetic nature of the prepared Zn-doped *C. roseus* extract, and this was compared with a standard drug (Acarbose). The results showed that the biosynthesized NPs had encouraging inhibitory effects on the alpha-amylase (α-1,4-glucan-4-glucanohydrolase) enzyme. Therefore, the significant results of this work are the generation of value-added drugs from the *C. roseus* plant for biotechnology and nanomaterial-based industries.

Received 12th September 2020,
Accepted 9th November 2020

DOI: 10.1039/d0ma00698j

rsc.li/materials-advances

1. Introduction

In recent years, the use of green NPs has been addressed in playing a significant role in medicine, agriculture and solar cell fields. Therefore, obtaining new synthesis methods using biological systems for the fabrication of nanoparticles can pave a promising pathway for biomedical and nanotechnology-based industries.[1–4] Researchers have carried out investigations to explore a low-environmental impact method for developing well-characterized NPs. Different low-cost and low-environmental impact approaches for preparing NPs have emerged as alternatives to traditional synthetic processes.[5] One of the most considered techniques is the synthesis of NPs using organisms. Among all organisms, plants appear to be the best candidates for this and they are appropriate for the up-scaled bio-production of NPs.[6] NPs synthesized by extracts are more stable and the rate of production is faster than in the case of microorganisms. In addition, extracts of medicinal plants are often utilized as stabilizing and reducing materials in the production of metallic NPs.[7–9]

The green preparation of NPs using extracts of medicinal plants has been employed to control the shapes of biosynthesized NPs, which determines their optical and biological features.[10–14] In this regard, green NPs have been produced in recent years using diverse plants such as neem, alfalfa, *Emblica Officinalis*, lemongrass, tamarind, and *Euphorbiatirucalli*.[15] Azeez and co-workers reported the biosynthesis of ZnO NPs using *Punica granatum* (pomegranate) juice extract as an efficient chelating and capping agent.[16] In another study, ZnO NPs were prepared in a green method, employing *Eucalyptus globulus* Labill. leaf extract and zinc nitrate hexahydrate salt, and this showed good merits for possible medical applications.[17] Himdad and co-workers reported the biosynthesis of ZnO NPs employing the *Apium graveolens* L. leaf plant and the prepared ZnO NPs revealed good properties for removing organic pollutants.[18] Among plants, *C. roseus* is an important medicinal

[a] *Department of Physics, Periyar University, P.G. Extension Center, Dharmapuri, Tamil Nadu, India*
[b] *Department of Physics, Jayam Arts and Science College, Dharmapuri, Tamil Nadu, India*
[c] *Technical Engineering College, Middle Technical University, Baghdad 100001, Iraq. E-mail: mustafa_kareem97@yahoo.com; Tel: +9647719047121*

plant distributed throughout the world that can be utilized to synthesize NPs from metal solutions and can serve as an excellent nano-factory. The attention towards this extract is due to the fact that it possesses monomeric indole alkaloids: vindoline and catharanthine, as its most abundant constituents, and these have important medicinal values.[19] Therefore, this material has considerable pharmacological merits such as antifungal,[20] anticancer,[21] antioxidant[22] and antibacterial activities.[23] Hence, it is highly suitable to produce effective eco-friendly NPs from the *C. roseus* plant without the addition of hazardous acid solvent, surface passivation chemicals or a difficult post-treatment process.

Amongst the NPs, ZnO-NPs exhibit considerable semiconducting merits because of their high exciton binding energy and the fact that they possess a wide bandgap at 3.37 eV, and so can be used for optical, biological, gas sensing and medical applications. Furthermore, they are employed by industries, such as in wastewater treatment, and as pharmaceutical products for drug delivery, with anti-cancer, anti-diabetic, and antibacterial activities, as well as anti-fungal properties.[24–29] However, the drawbacks of the toxicity of ZnO-NPs towards biological systems remains a controversial problem within recent reports.[30] We believe that nanotechnology will dramatically improve the evolution of medicine.

Notably, no previous study has been reported in the literature on the biosynthesis of Zn-doped *C. roseus*. The present study was designed in a facile, eco-friendly manner, and it was cost-effective in the synthesis of Zn-doped *C. roseus* NPs using the *C. roseus* extract as a green precursor, and we have investigated the anti-diabetic activities of the NPs. The oxygen functional groups, size and crystallinity of Zn-doped *C. roseus* were recorded by FTIR, TEM, and XRD. Our findings showed that *C. roseus*-based Zn NPs have high anti-diabetic activity.

2. Experimental

2.1. Materials

A fresh part of *C. roseus* was collected from the Dharmapuri area of Agragaram, Dharmapuri District, Tamilnadu, India. Zinc sulfate monohydrate (99%, $ZnSO_4$), α-amylase, acarbose, iodine, and hydrochloric acid (HCl) were ordered from Sigma-Aldrich. Distilled water (DW) was provided from Evergreen EG Laboratory, Chennai in India.

2.2. Preparation of green NPs

Zn-doped *C. roseus* NPs were biosynthesized using PIM. In brief, fresh *C. roseus* extracts were cleaned with DW and ground up. Then, 30 g of the *C. roseus* fine plant solution and 3 g of $ZnSO_4$ were added to 1000 ml of DW. The mixed dispersion was stirred for 5 days under a 500 W Halogen light and then kept in an air atmosphere for 20 days under solar light. Finally, the collected powder was dried and calcinated at 100 °C for 1 h.

2.3. Characterization

The XRD pattern of the NPs was recorded on a Bruker D8 Advance powder diffractometer with Cu Kα (λ = 0.15406 nm) radiation. The shape, size, and elemental composition were visualized using field emission scanning electron microscopy (FESEM, Hitachi S-4800), TEM (JEM-2100F), and EDX, respectively. The FTIR pattern of the NPs was measured using a KBr pellet approach on a Bruker Tensor 27 spectrometer. *Z*-Average and zeta potential measurements were recorded using dynamic light scattering (DLS) analysis (Horiba). Ultraviolet-visible diffuse reflectance spectroscopy (UV-DRS) of the sample was determined with a PerkinElmer Lambda 25 spectrophotometer.

2.4. Alpha-amylase assay

The α-amylase inhibitory effect of the green NPs (Zn-doped *C. roseus*) was performed using the standard protocol with little modification.[31] First, 100 μl of α-amylase material (0.1 mg ml^{-1}) was mixed with various amounts (10, 20, 40, 80, 160, and 320 μg ml^{-1}) of the green NPs, a standard (acarbose), and a control (without standard/test samples), and the samples were then pre-incubated at 37 °C for 20 min. 100 μl of starch solution was added to initiate the reaction and the samples were incubated at 37 °C for 60 min. Subsequently, 10 μl of 1 M HCl and 100 μl of iodine were added to the reaction tubes. The absorbance values of the dispersions were recorded at 580 nm and the α-amylase inhibitory effect was evaluated using the following equation:[31]

$$\% \text{ of Inhibition} = [(\text{OD of test} - \text{OD of control})/\text{OD of test}] \times 100$$

3. Results and discussion

The crystal nature of Zn-doped *C. roseus* NPs was determined by XRD patterns, as shown in Fig. 1a. The XRD was performed in the range of 10–70° and most of the diffraction peaks can be attributed to Zn-doped *C. roseus* NPs, according to previous reports.[32] The broadening of the peaks implies the fabrication of Zn-doped *C. roseus* NPs within the nanometer range.[33] XRD results corroborated well with those in previously reported literature.[34] The highest intensity peak of the Zn-doped *C. roseus* NPs along with other smaller intensity peaks were observed. The average particle size of the Zn-doped *C. roseus* NPs was found to be 16 nm, using Debye Scherrer's formula.[35] These XRD findings prove the purity of the synthesized Zn-doped *C. roseus* NPs. An FTIR spectroscopic study (Fig. 1b) was carried out to investigate the plausible mechanism behind the formation of Zn-doped *C. roseus* NPs. As can be seen, the FTIR shows the availability of functional groups at 3420 cm^{-1}, corresponding to the O–H stretch of H–bonded amino acids, and at 2848 cm^{-1} for the O–H stretching of the $-CH_2$ groups. The absorption bands were centered at wavenumbers of 2922 cm^{-1} and 1630 cm^{-1}, corresponding to the vibrational stretches of C–H and the carboxyl groups (asymmetrical COO^- stretching vibration), respectively, and at 1410 cm^{-1} due to the symmetrical COO^- stretching vibration.[36] Very weak bands

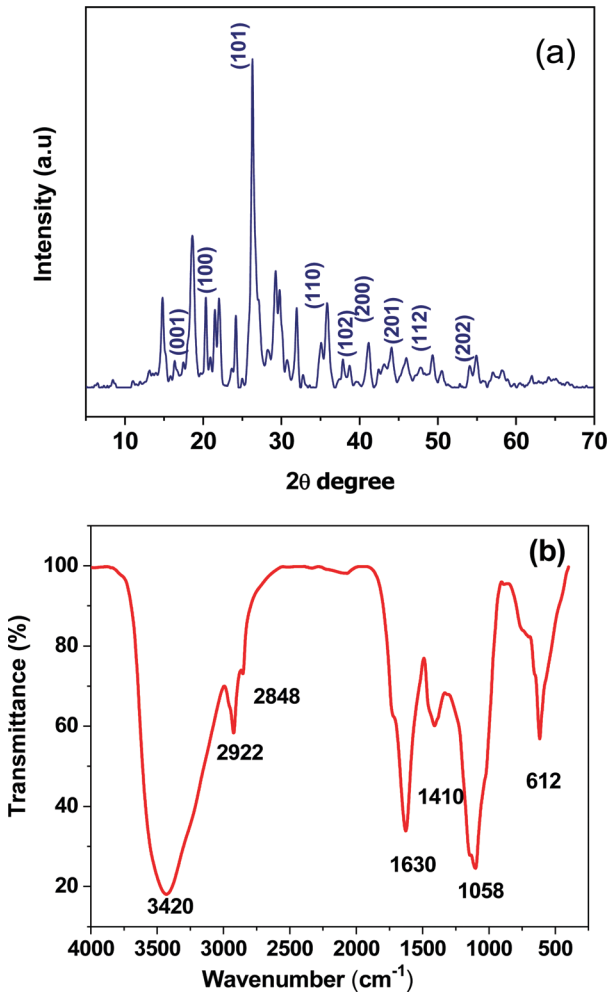

Fig. 1 (a) XRD spectrum of the green synthesized Zn-doped *C. roseus* NPs. (b) FTIR spectrum of the Zn-doped *C. roseus* NPs.

centered at 1058 cm^{-1} correspond to C–O stretched aromatic amines and aliphatic amines.[37] The plant extract serves as a reducing and stabilizing material in the conversion of the plant to green NPs. The strong absorption band at 612 cm^{-1} is due to the Zn-doped *C. roseus* NPs.[38–41] The functional groups present in the plant extract contribute to the mechanism of bonding within the Zn NPs. Any shift or change in the location or intensity of the bands in the spectra of the NPs can be correlated with the interaction of the oxygen agents of the plant extract with the Zn NPs. It can therefore be deduced that oxygen agents in the plant donate electrons that can reduce Zn ions and finally obtain the Zn NPs. In addition, the negative oxygen groups present in the plant can have a stabilizing effect.

The zeta potential value was determined to be −0.8 for the Zn-doped *C. roseus* NPs, as shown in Fig. 2. The zeta potential value provides us with evidence regarding the surface charge of the NPs, and this appeared to be more negative than previously reported.[42–44] Additionally, it gives us an idea about the stability of the NPs and the zeta potential value obtained for the Zn-doped *C. roseus* NPs lies within the low

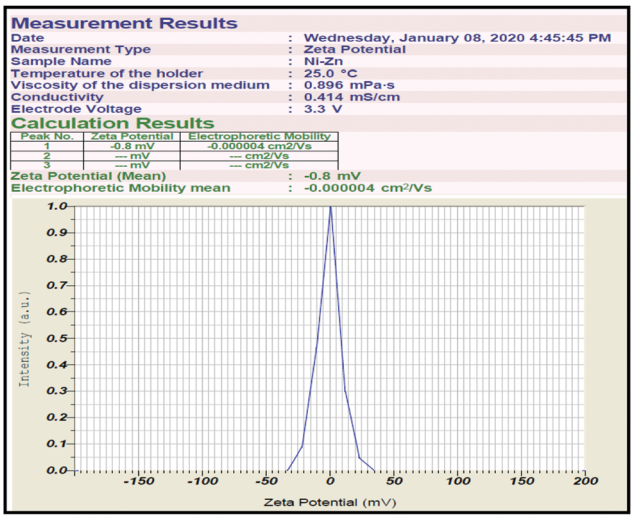

Fig. 2 Zeta potential analysis of the Zn-doped *C. roseus* NPs.

stable range, implying that the green NPs are unstable in aqueous solution. Therefore, there may be possible aggregations due to residual surfactants.

The UV-DRS reflectance spectrum of Zn-doped *C. roseus* is shown in Fig. 3a. The bandgap energy of the prepared NPs was obtained using a Tauc plot (Fig. 3b).[45] This demonstrated that the measured bandgap energy of the NPs is an indirect type with a value of 2.74 eV. The narrow bandgap in the Zn-doped *C. roseus* NPs, obtained by PIM, may be assigned to the upward shifting of the valence band. Therefore, it can be concluded that a smaller bandgap is more important for visible light absorption.

The morphology of the Zn-doped *C. roseus* NPs was studied using FESEM and the results are shown in Fig. 4a. It can be seen that the surface of the sample appears uneven due to the domination of the co-precipitate of the metal with the plant. The particles are random in size and are irregular in shape. The FESEM image of the Zn-CR NPs exhibited sizes ranging between 15 and 20 nm, proving the existence of spherical Zn-doped *C. roseus* NPs (red circular area). The TEM image of the Zn-doped *C. roseus* NPs is presented in Fig. 4b. As observed, the TEM image shows agglomerated globular NPs. In addition, the results demonstrated that the biosynthesized NPs in this work are multi-dispersed with a particle size range of 10–20 nm. The extremely small particle size can obtain great specific surface area and surface energy. No mono-dispersion of NPs was observed. Due to the high surface energy, *C. roseus* NPs in an aqueous medium tend to form agglomerates.

Fig. 5 shows the elemental analysis of the Zn-doped *C. roseus* NPs using EDX mapping. The weight percentages of C, O, S, K, Ca, and Zn were 45%, 21%, 13%, 6%, 5% and 10%, respectively. These results confirm that a very small amount of Zn is present.

The α-1,4-glucan-4-glucanohydrolase is one of the most prominent secretory products of the pancreas and salivary gland. This is responsible for the hydrolysis of complex carbohydrates into oligosaccharides and disaccharides in the intestinal mucosa. These sugars are further digested to monosaccharides by the

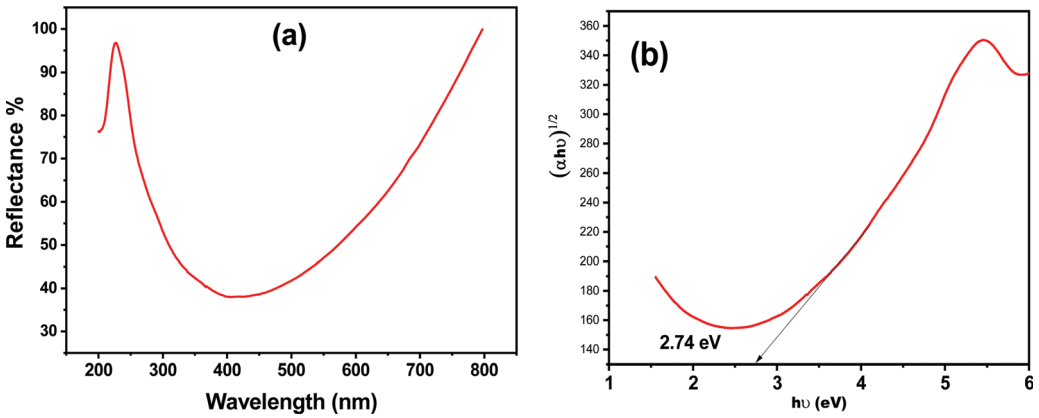

Fig. 3 UV-DRS measurements of (a) reflectance and (b) the indirect bandgap of the Zn-doped *C. roseus* NPs.

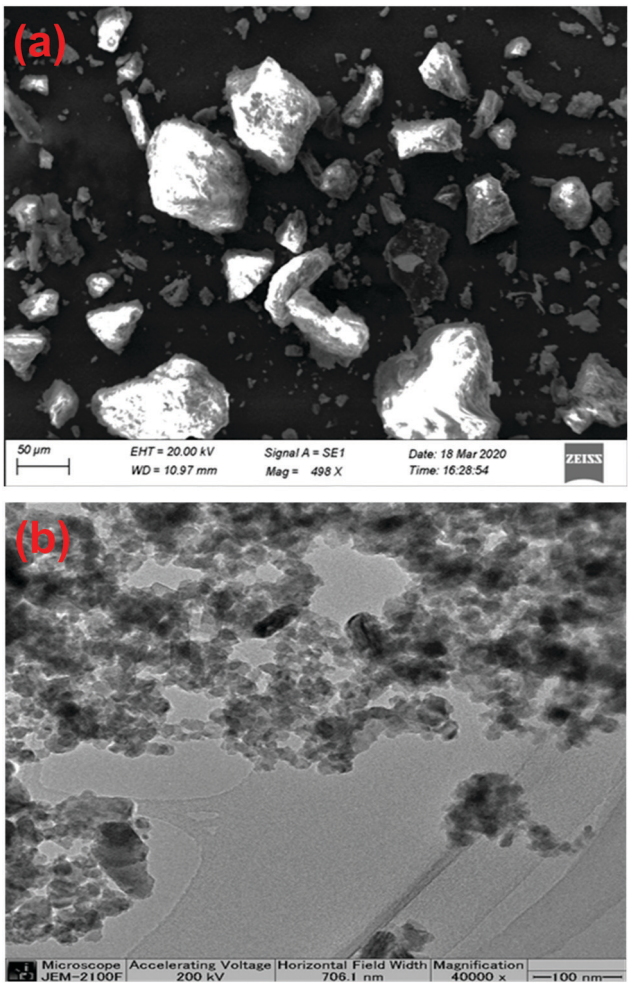

Fig. 4 (a) FESEM and (b) TEM images of the Zn-doped *C. roseus* NPs.

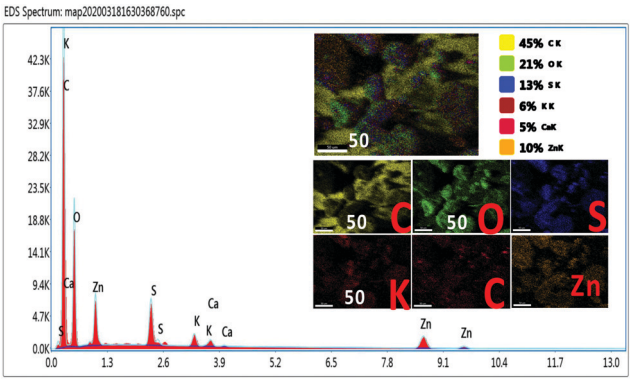

Element	Weight %	Atomic %	Net Int.	Error %	Kratio	Z	A	F
C K	55.87	69.12	3947.08	7.16	0.2292	1.0466	0.3919	1.0000
O K	27.85	25.87	1626.59	9.29	0.0573	1.0016	0.2053	1.0000
S K	3.92	1.82	812.87	2.14	0.0333	0.8920	0.9444	1.0077
K K	1.58	0.60	243.28	3.39	0.0135	0.8446	0.9920	1.0219
CaK	1.01	0.38	133.85	4.69	0.0089	0.8600	0.9967	1.0266
ZnK	9.75	2.22	366.72	3.21	0.0770	0.7314	1.0085	1.0706

Fig. 5 EDS spectrum and inset of the mapping images, and the Smart Quant Results of the Zn-doped *C. roseus* NPs.

action of alpha-glucosidase. The α-amylase inhibitory studies performed in the Zn-doped *C. roseus* extract showed moderate inhibitory potential, as shown in Fig. 6a and b. The half maximal inhibitory concentration (IC_{50}) value of the Zn-doped *C. roseus* extract is shown to have good α-amylase inhibitory activity. The IC_{50} value of the given sample was found to be 35.64165 μg ml^{-1}, whilst the value of the standard drug (Acarbose) was 13.085434 μg ml^{-1}. Herein, Zn serves as an actuator for blood sugar regulation, which is significantly affected in the presence of the Zn-doped *C. roseus* extract. The prepared Zn-doped *C. roseus* extract reveals an improved inhibitory effect for the treatment of diabetic issues and suppresses the fasting blood glucose level efficiently, due to the presence of amino acids in the Zn-doped *C. roseus* NPs.[46] Thus, biosynthesized Zn-doped *C. roseus* NPs can form an effective starch blocker drug to treat this dysfunction. Many synthetic medicines have certain side effects such as abdominal bloating and diarrhea. According to the above findings, stable and biocompatible Zn NPs associated with insulin

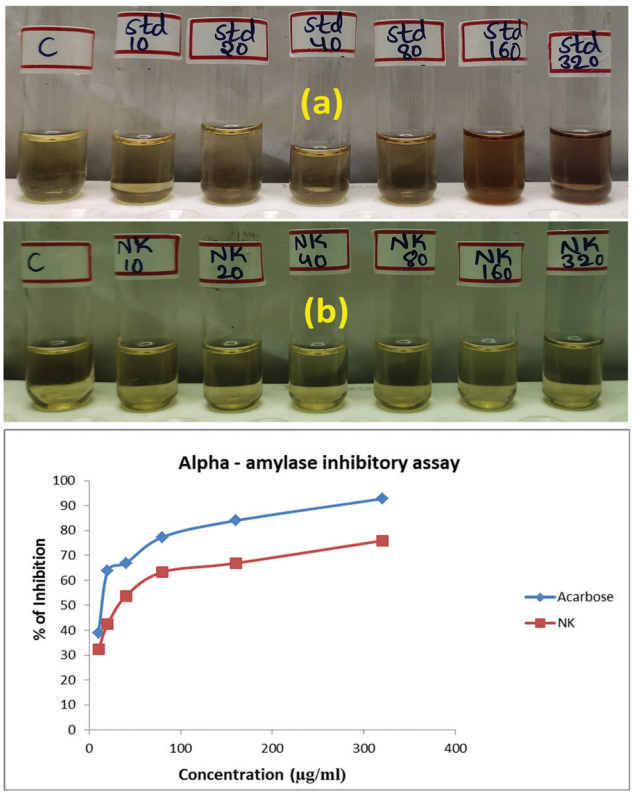

Fig. 6 (a) Anti-diabetic activity of the standard and of (b) the Zn-doped *C. roseus* NPs.

metabolism could be efficiently employed as a vital anti-diabetic drug.

4. Conclusion

Herein, we report a simple, green, and reproducible process for the environmentally-friendly preparation of a Zn-doped *C. roseus* plant for next-generation green biomedicine. As shown from the analytical results, the prepared Zn-doped *C. roseus* NPs had spherical morphology with a size of 10–20 nm, albeit in an aggregated form. In addition, the XRD results confirmed the production of crystalline NPs with a crystallite size of 16 nm. Herein, the biosynthesized NPs were tested for possible medical applications as anti-diabetic drugs. The Zn-doped *C. roseus* NPs showed good α-amylase inhibitory activity compared to the standard drug. Overall, it was clearly evident from our studies that Zn-doped *C. roseus* NPs can elicit potent anti-diabetic activity. Furthermore, these green NPs had no side effects compared with the standard sample. From the above results, we recommend that the biogenically synthesized green NPs can be used for different biological purposes, particularly in diabetes research.

Conflicts of interest

The authors declare no competing financial interest.

Acknowledgements

The authors thank Director Dr P. Mohana Sundram, PG Extension Centre, Periyar University, Dharmapuri-636107, Tamil Nadu, India.

References

1 P. Zibin, L. Yuman, S. Binoy, O. Gary and C. Zuliang, *J. Colloid Interface Sci.*, 2020, **558**, 106–114.
2 B. N. Rashmia, F. H. Sujatha, B. Avinashc, C. R. Ravikumarc, H. P. Nagaswarupad, M. R. A. Kumarc, K. Gurushanthae and M. S. Santoshf, *Inorg. Chem. Commun.*, 2020, **111**, 107580.
3 D. S. Ahmed, M. K. A. Mohammed and S. M. Majeed, *ACS Appl. Energy Mater.*, 2020, DOI: 10.1021/acsaem.0c01896.
4 M. Shakibaie, A.-E.-A. Fatemeh, A.-S. Mahboubeh, A. Atefeh, D. Mohsen, F. Hamid and A. Alieh, *Nanomed. J.*, 2019, **6**, 223–231.
5 K. S. Virender, A. Y. Ria and L. Yekaterina, *Adv. Colloid Interface Sci.*, 2009, **145**, 83–96.
6 P. Horky, S. Sylvie, U. Lenka, B. Daria, K. Silvia, B. Zuzana and K. Eliska, *J. Anim. Sci. Biotechnol.*, 2019, **10**(1), 17.
7 B. Aderibigbe, *Molecules*, 2017, **22**, 1370.
8 M. A. Albrecht, C. W. Evans and C. L. Raston, *Green Chem.*, 2006, **8**, 417.
9 M. Anbuvannan, M. Ramesh, G. Viruthagiri, N. Shanmugam and N. Kannadasan, *Mater. Sci. Semicond. Process.*, 2015, **39**, 621–628.
10 N. Bala, S. Saha, M. Chakraborty, M. Maiti, S. Das, R. Basu and P. Nandy, *RSC Adv.*, 2014, **5**, 4993–5003.
11 G. Bhumi and N. Savithramma, *Int. J. Drug Dev. Res.*, 2014, **6**, 208–214.
12 T. Bhuyan, K. Mishra, M. Khanuja and R. Prasad, *Mater. Sci. Semicond. Process.*, 2015, **32**, 55–61.
13 M. Gupta, R. S. Tomar, S. Kaushik and R. K. Mishra, *Front. Microbiol.*, 2018, **9**, 1–13.
14 S. K. Chaudhuri and L. Malodia, *Appl. Nanosci.*, 2017, **7**(8), 501–512.
15 H. R. Naika, K. Lingaraju, K. Manjunath, D. Kumar, G. Nagaraju, D. Suresh and H. Nagabhushana, *J. Taibah Univ. Sci.*, 2014, 4–6.
16 A. B. Azeez, M. H. Samir, M. E. Mahera, K. A. Semih and H. S. H. Faiq, *Micro Nano Lett.*, 2020, **15**, 415–420.
17 A. B. Azeez and H. A. Himdad, *SN Appl. Sci.*, 2020, **2**, 991.
18 H. A. Himdad and A. B. Azeez, *Desalin. Water Treat.*, 2020, **190**, 179–192.
19 M. T. Ansari, S. Farheen, A. K. Fatin, Z. A. Mohammad, A. S. Tengku, M. bin Tengku, M. Shahnaz and A. Sadath, *Curr. Nanomed.*, 2018, **8**, 225–233.
20 S. Roy and P. Chatterjee, *Ind. Crops Prod.*, 2010, **32**, 375–380.
21 S. Gajalakshmi, S. Vijayalakshmi and V. Devi Rajeswari, *Int. J. Pharma Biol. Sci.*, 2013, **4**, 821–830.
22 D. M. Pereira, J. Faria, L. Gaspar, F. Ferreres, P. Valentão, M. Sottomayor and P. B. Andrade, *Food Chem.*, 2010, **121**, 56–61.
23 A. B. Azeez, M. H. Samir and J. I. Haidar, *Eurasian J. Sci. Eng.*, 2019, **4**, 74–83.

24 H. Pavel, S. Sylvie, U. Lenka, B. Daria, K. Silvia, B. Zuzana, K. Eliska, L. Zuzana, C. Natalia, G. Milica, M. Vedran, S. Vendula, V. Eva, N. Pavel, K. Pavel, K. Olga, H. David, K. Pavel, S. Jiri, A. Vojtech and S. Kristyna, *J. Anim. Sci. Biotechnol.*, 2019, **10**, 17.
25 S. Divyapriya, C. Sowmia and S. Sasikala, *World J. Pharm. Pharm. Sci.*, 2014, **3**, 1635–1645.
26 R. Dobrucka and J. Długaszewska, *Saudi J. Biol. Sci.*, 2016, **23**, 517–523.
27 R. Farzana, P. Iqra, F. Shafaq, S. Sumaira, K. Zakia, T. Hunaiza and M. Husna, *Arch. Clin. Microbiol.*, 2017, **8**, 57.
28 K. A. M. Mustafa, *Optik*, 2020, **217**, 164867.
29 K. A. M. Mustafa, S. A. Duha and R. M. Mohammad, *Mater. Res. Express*, 2019, **6**, 055404.
30 J. Jinhuan, P. Jiang and C. Jiye, *Bioinorg. Chem. Appl.*, 2018, **2018**, 1–18.
31 J. O. Unuofin, G. A. Otunola and A. J. Afolayan, *Heliyon*, 2018, **4**(9), e00810.
32 M. Gupta, R. S. Tomar, S. Kaushik, R. K. Mishra and D. Sharma, *Front. Microbiol.*, 2018, 9.
33 S. P. Rajendran and K. Sengodan, *J. Nanosci.*, 2017, **2017**, 1–7.
34 H. N. Fal and F. Farzaneh, *J. Sci., Islamic Repub. Iran*, 2006, **17**(3), 231–234.
35 K. A. M. Mustafa, *Plasmonics*, 2020, DOI: 10.1007/s11468-020-01224-5.
36 S. A. Duha and K. A. M. Mustafa, *Chem. Pap.*, 2020, **74**, 4033–4046.
37 R. M. Mohammad, D. S. Ahmed and K. A. M. Mustafa, *J. Sol-Gel Sci. Technol.*, 2019, **90**, 498–509.
38 G. Nagaraj, D. Brundha, V. Kowsalya, C. Chandraleka, S. Sangavi, R. Jayalakshmi, M. Arulpriya, N. Sathya, M. Prasath and S. Tamilarasu, *Mater. Today Proc.*, 2020, DOI: 10.1016/j.matpr.2020.05.318.
39 P. Jithendra, A. M. Rajam, T. Kalaivani, A. B. Mandal and C. Rose, *ACS Appl. Mater. Interfaces*, 2013, **5**(15), 7291–7298.
40 F. Nejatzadeh-Barandozi and S. Enferadi, *Org. Med. Chem. Lett.*, 2012, **2**(1), 33.
41 O. Saibuatong and M. Phisalaphong, *Carbohydr. Polym.*, 2010, **79**(2), 455–460.
42 M. Singh Rajput, V. Nair and A. Chauhan, *Middle East J. Sci. Res.*, 2011, **7**(5), 784–788.
43 P. P. Pillay, C. P. M. Nair and T. N. Santi Kumari, *Bull. Res. Inst., Univ. Kerala, Trivandrum, Ser. A*, 1959, **1**, 51–54.
44 S. Chakraborty, N. Kar, L. Kumari, A. K. De and T. Bera, *Int. J. Nanomed.*, 2017, **12**, 4849–4868.
45 S. A. Duha, R. M. Mohammad and K. A. M. Mustafa, *Nanosci. Nanotechnol.*, 2020, **10**, 127–133.
46 D. J. Manasa, K. R. Chandrashekar, A. P. K. Masineni, S. Doddavenkatanna, P. Ashwini, P. D. Rekha and S. Sana, *Appl. Nanosci.*, 2020, **10**, 3057–3074.